SCIENTIFIC REPORTS

OPEN

Improvement of a rapid diagnostic application of monoclonal antibodies against avian influenza H7 subtype virus using Europium nanoparticles

Seon-Ju Yeo[1], Duong Tuan Bao[1], Ga-Eun Seo[2], Cuc Thi Bui [1], Do Thi Hoang Kim[1], Nguyen Thi Viet Anh[1], Trinh Thi Thuy Tien[1], Nguyen Thi Phuong Linh[1], Hae-Jin Sohn[2], Chom-Kyu Chong[3], Ho-Joon Shin[2] & Hyun Park[1]

The development of a sensitive and rapid diagnostic test is needed for early detection of avian influenza (AI) H7 subtype. In this study, novel monoclonal antibodies (mAbs) against influenza A H7N9 recombinant hemagglutinin (rHA)1 were developed and applied to a Europium nanoparticle–based rapid fluorescent immunochromatographic strip test (FICT) to improve the sensitivity of the rapid diagnostic system. Two antibodies (2F4 and 6D7) exhibited H7 subtype specificity in a dot-FICT assay by optimization of the conjugate and the pH of the lysis buffer. The subtype specificity was confirmed by an immunofluorescence assay and Western blot analysis. The limit of detection of the FICT employing novel mAbs 31 ng/mL for H7N9 rHA1 and 40 hemagglutination units/mL for H7 subtype virus. Sensitivity was improved 25-fold using Europium as confirmed by comparison of colloidal gold-based rapid diagnostic kit using the 2F4 and 6D7 mAbs.

Recurrence of highly pathogenic avian influenza A (HPAI) virus H7 subtype in humans and poultry continues to be a serious concern to public health[1]. Prior to 2003, outbreaks of avian influenza (H7N1 and H7N3) occurred in poultry in Europe. Since then, human-to-human transmission HPAI virus (H7N7) has been reported. An outbreak in the Netherlands infected 89 people[2–6]. In 2013, an outbreak of H7N7 resulted in the culling of more than 1 million chickens[7]. Three of 200 workers involved in the cull developed conjunctivitis despite strict infection control procedures that were in place. Another HPAI virus H7 subtype that infects humans is avian influenza A (H7N9). The first H7N9 outbreak occurred in China in 2013. Most recently, an outbreak resulted in about 400 human cases in China, Hong Kong and Taiwan, with a mortality rate of 27–36%[8–10]. Airborne transmission of the subtypes H7N1, H7N7, and H7N9 has been reported[11–13]. H7 subtype virus infection is very contagious in poultry and humans, and is an immediate threat to public health[14].

Avian influenza A virus infection in humans cannot be typically diagnosed by clinical signs and symptoms alone. Laboratory testing is required. A guideline of the United States Centers for Disease Control and Prevention (CDC) recommends molecular detection methods like real-time reverse transcription-polymerase chain reaction (rRT-PCR) for the laboratory diagnosis of influenza infections and hemagglutinin (HA) subtype identification is preferred[15]. Although rapid point-of-care detection tests (POCT) are not generally performed for avian influenza because the low sensitivity to detect AI virus, several studies have sought to develop H7 subtype-sensitive[16] or specific[17] POCT; such tests would be convenient to use on-site during outbreaks. But, the development of H7-specific POCT has been hindered by the high labor costs to develop the specific antibody test and the

[1]Zoonosis Research Center, Department of Infection Biology, School of Medicine, Wonkwang University, 460, Iksan-daero, Iksan, 54538, Republic of Korea. [2]Department of Microbiology, Ajou University School of medicine, and Department of Biomedical Science, Graduate School of Ajou University, Suwon, Republic of Korea. [3]GenBody Inc, No. 206, Biotech Business IC, DanKook University, San-29, Anseo-dong, Dongnam-gu, Cheonan, Republic of Korea. Seon-Ju Yeo and Duong Tuan Bao contributed equally to this work. Correspondence and requests for materials should be addressed to H.-J.S. (email: hjshin@ajou.ac.kr) or H.P. (email: hyunpk@wku.ac.kr)
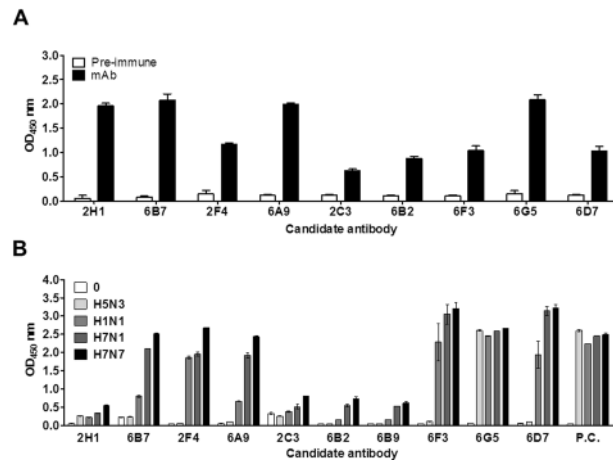
Figure 1. Development of H7 subtype-specific antibodies. The fusions were performed using mouse spleen cells inoculated with H7N9 virus rHA1. Ten hybridomas were produced. The secreted antibodies from each hybridoma were tested for recombinant antigen (H7N9 HA1 (**A**) and different influenza subtype virus (**B**) by indirect ELISA. Pre-immune, serum from a healthy mouse; P.C., positive control antibody (anti-influenza A nucleoprotein antibody).

difficulty in identifying an antibody that is sufficiently stable and maintains its antigen recognition functionality in non-optimal environments[18].

In this study, two novel H7 subtype-specific monoclonal antibodies (mAbs) were developed and combined with a fluorescence molecule. The mAbs were adapted to POCT to develop a rapid fluorescent immunochromatographic strip test (FICT) assay. The assay was capable of producing results in 15 minutes.

The FICT assay is attractive as a rapid diagnostic test because of its greatly improved sensitivity for influenza RDT[19–22]. Europium is a widely-used and efficient fluorescence material, which has been incorporated in rapid diagnostic tests[23, 24]. These tests require delicate biosensor equipment, such as microchip and microplate reader. Until now, no study has sought to apply the Europium to H7 subtype-specific rapid diagnostic test.

The present study introduces novel H7 subtype (H7N1 and H7N7)-specific mAbs and demonstrates their success in improving the performance of a FICT assay that utilizes Europium nanoparticles.

Results

Characterization of the mAbs.
After immunization of mice with H7N9 rHA1 antigen, 10 hybridoma cell lines producing mAb were established. The antibody amounts ranged from 0.5 to 2 OD according to an ELISA for H7N9 rHA1 antigen (Fig. 1A). Indirect ELISA with all 10 mAbs was conducted for four influenza A subtype virus (H1N1, H5N3, H7N1, and H7N7) at 1,000 HAU/mL. Reactivity of four clones (2H1, 2C3, 6B2, and 6B9) to virus was relatively lower than other clones, although they showed positive signals in recombinant antigen-mediated indirect ELISA (Fig. 1B).

Six mAbs (6B7, 2F4, 6A9, 6F3, 6G5, and 6D7) reacted with the H7N1 and H7N7 subtypes and with H1N1 virus. One mAb (6G5) reacted with all subtypes. As positive control, anti-influenza A nucleoprotein (NP) (3G6) was used for confirmation of the equal amount of each subtype virus; an OD of about 2.5 was produced in the presence of 1,000 HA units (HAU)/mL.

A dot-FICT assay was used to select the pair of H7 subtype-specific mAbs, mimicking the strip test (Fig. 2A). The broad detection (6G5) to 1,000 HAU/mL of each virus compelled its choice as the detection element. Five other mAbs (6A9, 6D7, 6F3, 6B7, and 2F4) with strong reaction to 1,000 HAU/mL of virus were dotted on the strip. The 6D7 mAb demonstrated the strongest reactivity with H7 subtypes with 6G5. The 6F3 and 2F4 mAbs, which had strong reactivity to virus, hardly reacted with 6G5, implying a shared epitope. As the strongest reactivity was observed by 6D7 for H7 subtypes, reactivity with other mAbs was examined to ascertain specificity (Fig. 2B). Further testing showed that three mAbs (6G5, 6F3, and 6B7) cross-reacted with H1N1 in addition to H7 subtypes. However, 2F4 showed the potential H7 subtype specificity with 6D7, showing strong reactivity to H7N1 and H7N7 virus. The 6A8 mAb failed to recognize H7N1 virus. The 2F4 and 6D7 mAbs were selected for subsequent experiments.

To further confirm the specificity, the viral reactivity of the mAbs was analyzed by Western blot assay and immunofluorescence assay (Fig. 3). Hybridoma cells were expanded in ascites and the purified antibody was confirmed by SDS-PAGE. The gels displayed two dominant bands at 50 kDa (heavy chain) and 25 kDa (light chain) (Fig. 3A). To assess the ability of these mAbs to recognize the linear epitope, 1,000 HAU/lane of virus was used for Western blot analysis. The 2F4 mAb reacted to both H7N1 and H7N7 subtypes (Fig. 3B). The 6D7 mAb did not react with linearized antigen, implying that this antibody would contribute to the specific reactivity through conformational structure of target antigen. In the immunofluorescence assay, the 2F4 and 6D7 mAbs both were reactive against the H7N1 and H7N7 virus subtypes and not against the other subtype tested (Fig. 3C). The positive signal of anti-influenza NP (3G6) showed the presence of virus in the two assays.
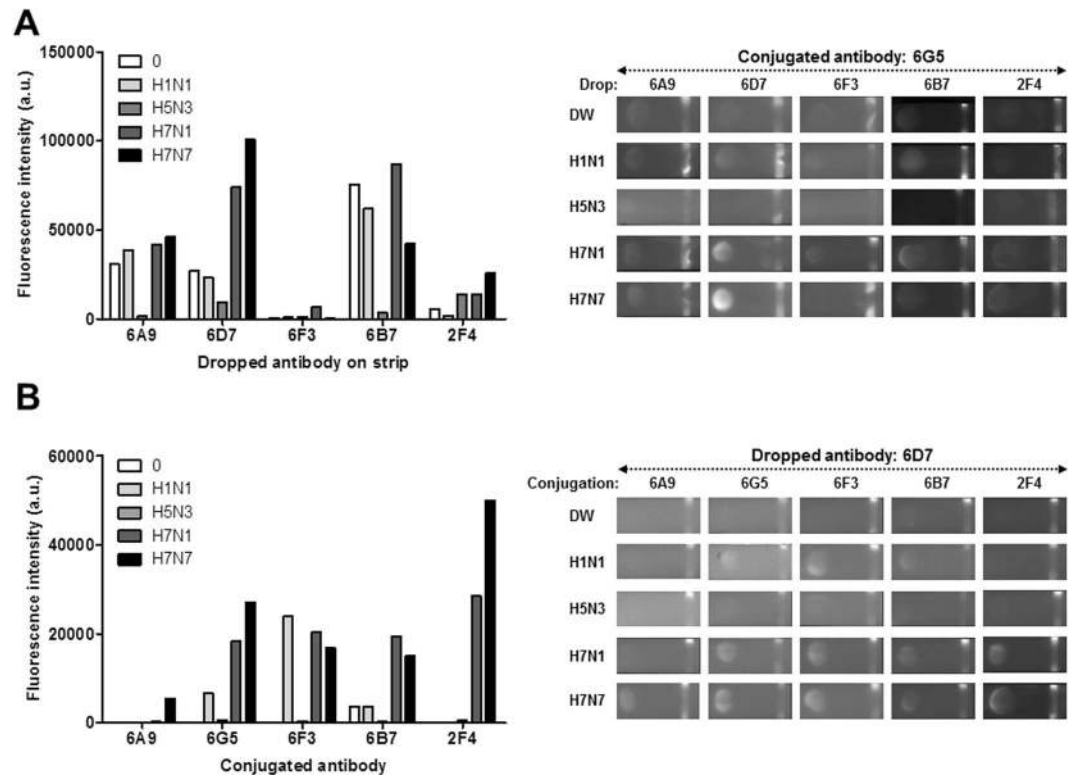
Figure 2. Monoclonal antibody (mAb) reactivities with different H7 virus strains and subtypes in the dot-FICT assay. Dot-FICT assays were used to examine the specificity of the mAbs against different AI virus subtypes and diverse H7 isolates. 6G5 was chosen as detection element and was conjugated with Europium. Five clones were used for dotting on strip and different virus subtypes were applied to the dot-FICT assay (**A**). 6D7 was chosen for dotting on strip and other antibodies were conjugated with Europium and dot-FICT assay was performed (**B**). Raw data for fluorescent image of dotting are shown in the right panel of each graph.

Optimization of FICT assay. Figure 4A schematically illustrates the Europium conjugate-based FICT assay. The test strip for FICT has a conjugate pad for conjugate and a sample pad for application of sample on a nitro-cellulose membrane. Anti-influenza H7 subtype-specific antibody (6D7) and anti-mouse IgG Abs were coated on the test line (TL) and the control line (CL) of the nitrocellulose membrane, respectively. To perform the diagnostic assay, the conjugates were loaded on the conjugation pad in advance. Virus in lysis buffer was applied to the sample pad. In the absence of virus, the conjugates failed to react with mAb in the TL. However, in the presence of virus, conjugate was on TL line. At the CL, anti-mouse IgG recognized the antibody on conjugate. After the application of sample to the strip, the fluorescence intensity was digitalized by the light-emitting diode-based portable strip reader in 15 min.

The optimal performance of the FICT assay was obtained using 1,000 HAU/mL of H1N virus and H7N7 virus. The dot-FICT did not showed cross-reactivity with the Abs when H1N1 was present at 1,000 HAU/mL (Fig. 4B).

Nonspecific reaction of bioconjugate was explored by using different amounts of bovine serum albumin (BSA, 0.3125–5%) in conjugate storage buffer. BSA at 5% was able to decrease the cross-reaction of H1N. This concentration was chosen for the bioconjugate, even though H1N1 cross-reactivity persisted.

Instead of the increasing BSA further, we tested different pHs (8–12) of lysis buffer. The cross-reaction of H1N1 was decreased with reactivity of H7N7 virus (Fig. 4C). The remaining cross-reaction of H1N1 was not significantly different at pH 12 but the reactivity of H7N1 was decreased at that pH. Therefore, we chose the lysis buffer of pH 11. The results indicate that lysis buffer plays a key role in the antigen-Ab environment in addition to helping the migration of samples on a nitrocellulose membrane without non-specific reaction.

FICT assay performance. Serial dilutions of H7N9 HA1 and H5N1 HA1 (15–500 ng/mL were used to determine the limit of detection (LOD) of the FICT assay, based on the limit of blank (LOB), as described previously[25]. The FICT displayed H7N9 HA1 reactivity with good correlation ($r^2 = 0.9826$), but no reactivity with H5N1 rHA1 (Fig. 5). LOD for H7N9 rHA1 was 31 ng/mL. The proposed diagnostic system targeted the HA1 H7 subtype.

To confirm the virus specificity, serial dilutions (20–640 HAU/mL) of the H1N1, H5N3, H7N1, and H7N7 subtypes were tested in FICT using a 2F4 (conjugate)/6D7 (strip) Ab pair. The proposed assay showed good linear regression for H7N1 virus ($r^2 = 0.9743$) and H7N7 virus ($r^2 = 0.9897$). However, it could not recognize the other two subtypes tested (Fig. 6A). LOD was 40 HAU/mL of two H7 subtypes. Therefore, the assay had H7 subtype specificity.
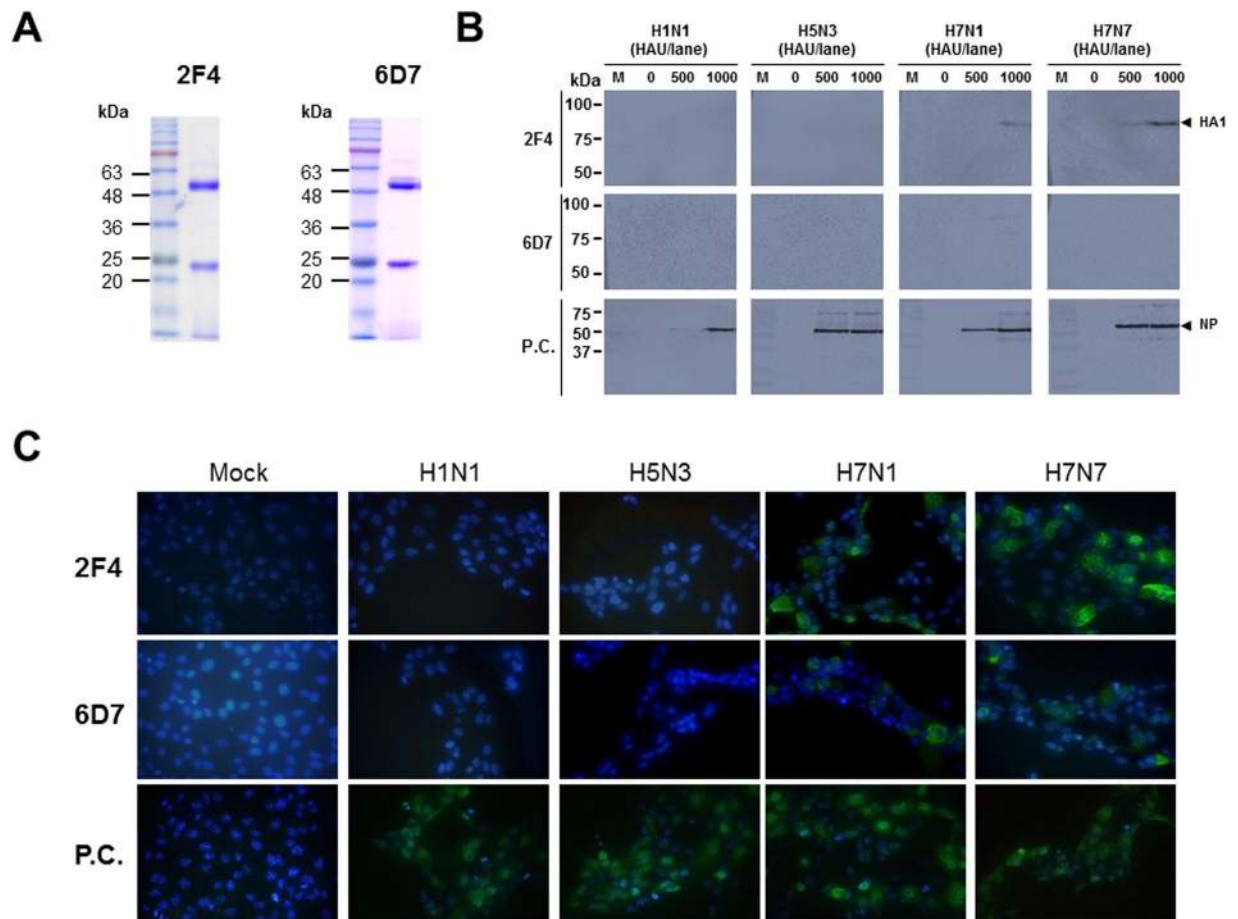
Figure 3. Characterization of H7 subtype-specific antibodies. Both 2F4 and 6D7 antibodies were produced in ascites and purified by Protein G and SDS-PAGE was conducted to identify the heavy - and light chain of each antibody (**A**). Four influenza A subtype viruses were loaded on a SDS-PAGE gel and Western blotting was used to analyze each antibody (**B**). In the immunofluorescence assay, cells were independently infected with the virus subtypes for 12 h, and the cells were fixed and incubated with 2F4 and 6D7 antibodies. After washing, fluorescence was detected by a FITC-conjugated secondary antibody (**C**). M, marker; Mock, no virus infection.

The RNA copy number of the LOD (40 HAU/mL) of FICT was determined (Fig. 6B). After preparing two-fold dilutions from of 10 HAU/mL to 80 plaque forming units (PFU)/mL of two H7 subtype viruses, 75 μL of sample was used for RNA extraction. Eluted RNA was used for rRT-PCR with the standard using plasmid dilution. To generate a calibration curve, serially-diluted RNA standard was used. A standard curve was drawn to show the starting copy number of the standard RNA vs the cycle threshold (Ct). RNA copy number/μL was determined by plasmid dilution as described previously[26]. The plot of a standard curve of Ct values against the logarithmic dilutions produced a r^2 value > 0.997 and the slope corresponded to efficiency in the range 87%, which was close to the optimized protocol. The 40 HAU/mL of H7N1 and H7N7 virus showed a Ct value of 30 and 31, respectively. The FICT RNA copy number LOD was 2.03×10^3 of RNA for H7N1 and 1.59×10^3 for H7N7.

The improved performance of the FICT assay was highlighted by comparison of RDT using colloidal gold nanoparticles. The 2F4/6DF Ab RDT showed a positive signal at 1000 HAU/mL of H7 subtype virus, but not with the other subtypes tested (Fig. 7A). This indicated that the fluorescent dye improved the performance of RDT by 25-fold. The conventional influenza A NP RDT displayed a LOD of 320, 160, 80, and 80 HAU/mL for H1N1, H5N3, H7N1, and H7N7 virus, respectively (Fig. 7B). The H7 subtype-specific FICT assay incorporating Europium nanoparticles markedly improved the performance of the RDT assay, surpassing the performance of the RDT detection of nucleoprotein, a highly expressed viral antigen, compared to HA.

Discussion

For a decade, many studies have sought to develop H7 subtype-specific rapid diagnostic immunoassays. Three ELISA-based H7 subtype- specific systems have been developed[27–29]. Recently, H7 subtype-specific Abs were reported to have vaccine efficacy[30, 31].

The LOD of the H7 rRT-PCR assay varies depending on primer, probe, and H7 subtype strain. Two reports achieved a LOD of 10^3–10^4 copies of H7 RNA[32, 33]. Using currently available probe and primers, Ct values of 35–37, corresponding to 20 and 200 copies per reaction, have been reported as the LOD of rRT-PCR of H7N1 virus[34].
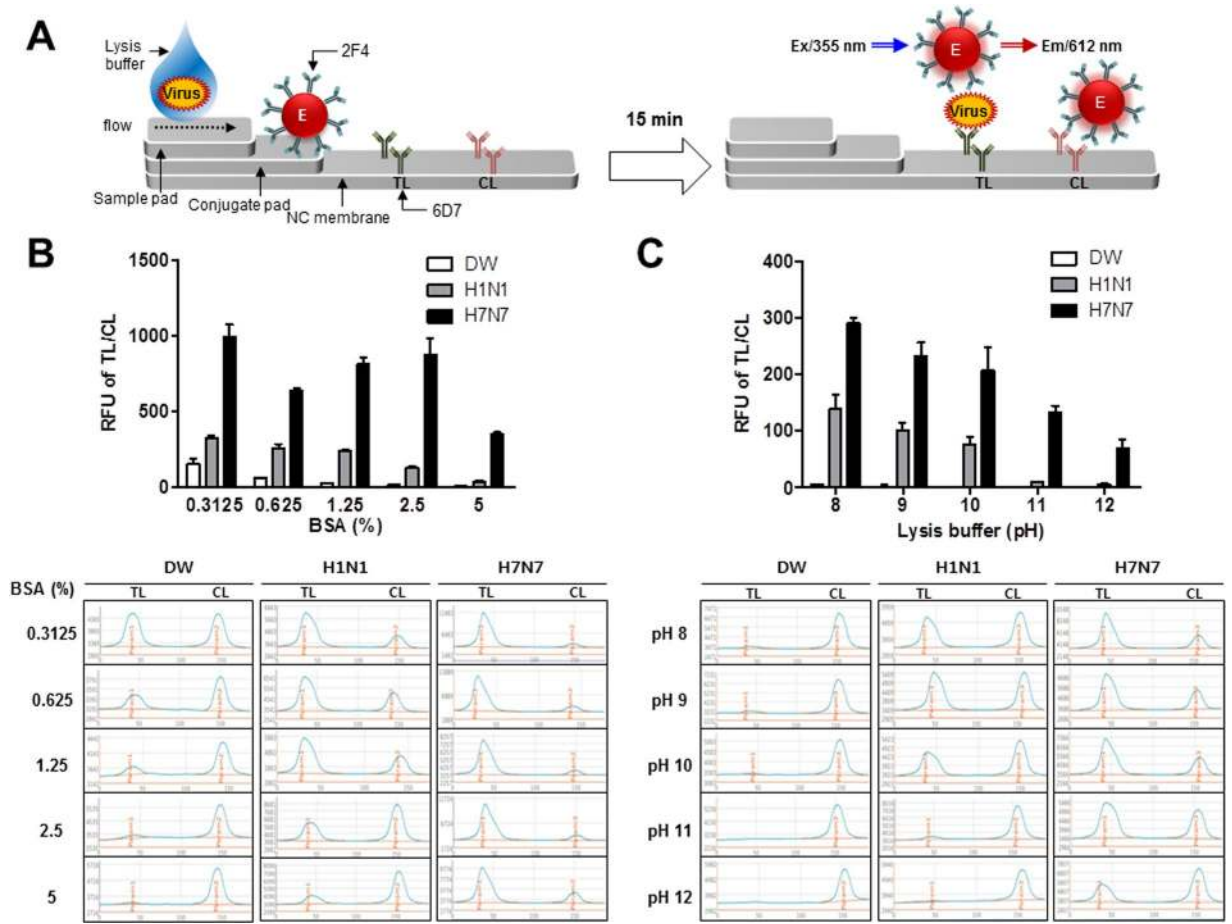
Figure 4. Optimization of FICT assay. Schematic diagram rapid fluorescence diagnostic system employing Europium-conjugated H7 subtype specific antibody was shown (**A**). 6D7 mAb was coated in the test line (TL) on NC membrane. Virus was pretreated with lysis buffer and Europium-conjugated antibody (2F4) was dropped onto the conjugate pad on the strip. Subsequently, sample was applied to the sample pad and after 15 min, the strip was used to detect the fluorescent light on the strip through the light emitting diode (LED)-built portable fluorescent strip reader. In the LED module, the excitation light (355 nm) was filtered by the emission filter (612 nm). To reduce nonspecific reactions of the FICT assay against H1N1 virus, different concentration of BSA was tested as a blocking agent to generate the bioconjugate (**B**). Lysis buffer was tested in different pH from 8 to 12 (**C**). All experiments were conducted in triplicate. The data are shown as mean ± SD. Raw fluorescence peaks from the test line (TL) and control line (CL) in FICT are shown in the bottom panel.

Until now, only two studies have reported on a H7 subtype-specific diagnostic system using novel mAbs. In one study, one HA unit of H7 was detected using an ELISA system[35]. The other study developed a H7 subtype-specific RDT and reported the LOD H7-specificity varied widely from Cts of 26–31 by rRT-PCR, depending on the isolates and strain of H7N9[17]. In our study, the LOD of the FICT assay achieved the latter, with a Ct of 30 for H7N1 and 31 for H7N7 by rRT-PCR. Therefore, our proposed FICT assay that utilizes fluorescent Europium performs better in term of average of Cts values.

The outstanding improvement of this FICT assay was highlighted by comparison of RDT using the colloidal gold nanoparticle-conjugated mAbs (2F4/6D7). This RDT was able to detect only 1,000 HAU/mL of H7 subtype virus when we applied the pair of these Abs.

NP is a well-conserved antigen, which has a role in encapsidation of viral RNA and which is used to identify the presence of influenza A or B virus in RDT systems because of the presence of multiple copies[36]. The surface-oriented glycoprotein HA antigen is a component of a subtype-specific protein.

Present results from Western blot analysis and immunofluorescence assay indicated HA expression in AI virus was detected at low level compared to that of NP. Therefore, the RDT LOD of 1,000 HAU/mL achieved using 2F4/6D7 could be partially due to the relatively low expression of HA.

The finding is reasonable compared to NP because a commercial influenza A/B kit targeting NP has a LOD of 80–320 HAU/mL all four subtype virus (Fig. 7B).

Additionally, the improvement of performance of FICT employing Europium was confirmed by FICT targeting NP (Figure S1). When we tested the Europium-conjugate with anti-influenza NP in FICT, LOD of RDT (LOD: 80 HAU/mL) was improved by 8-fold (LOD: 10 HAU/mL) in Europium-employing FICT assay. Therefore, our study supported that the low sensitivity of RDT could be improved by employing the fluorescence material. The
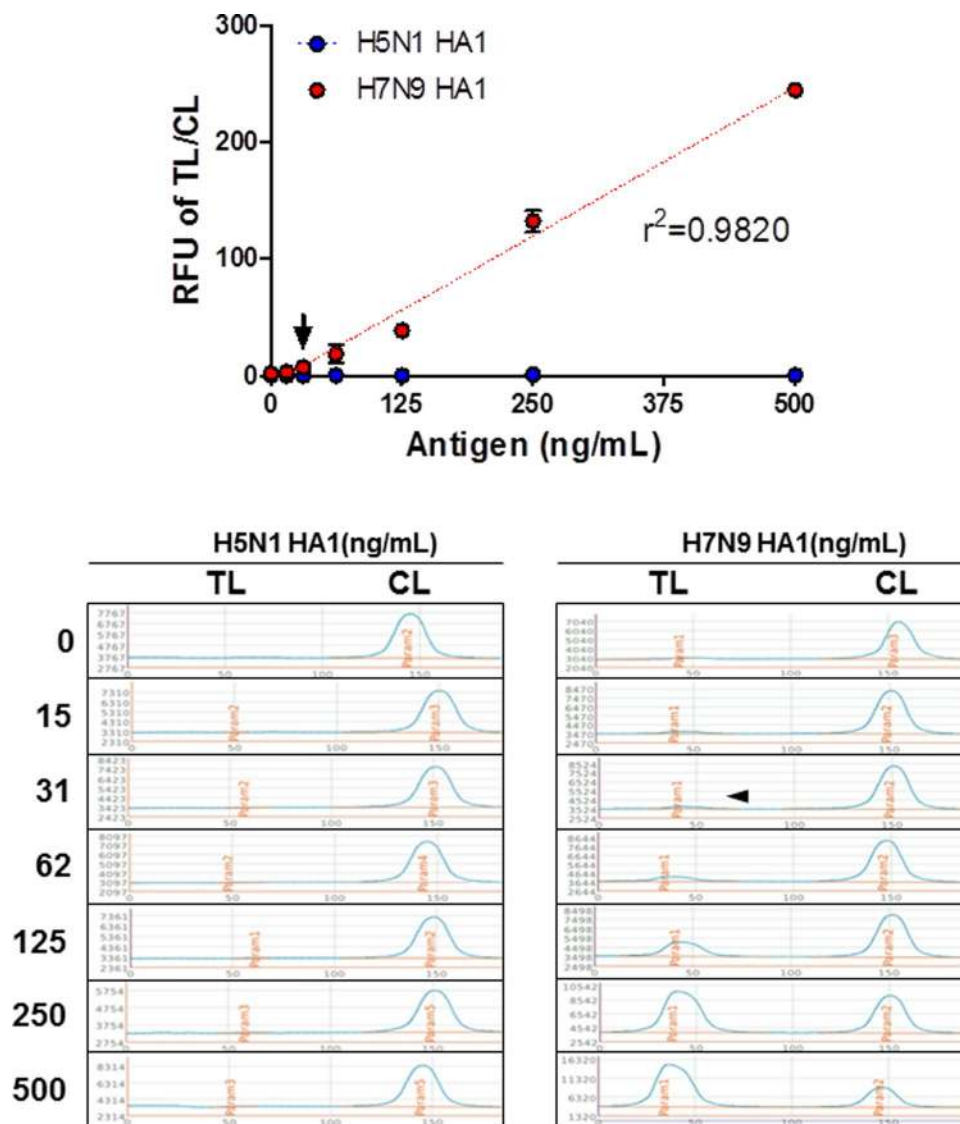
Figure 5. Detection limit of FICT assay for target antigen. FICT employing Europium-conjugated antibodies were tested for the limit of detection (LOD) against H7N9 rHA1 (**A**). The data ($n = 3$) are shown as mean ± SD. Linear regression is shown with the dotted line. The arrow indicates the antigen concentration of LOD. Raw fluorescence peaks from the test line (TL) and control line (CL) in FICT are shown in the bottom panel.

main challenge in the present study was to find a method that would be suitably able to improve the ability of the rapid diagnostic assay. We achieved this goal using Europium containing nanoparticles.

Although coupling of fluorescent dye to antibody has a good record of improving RDT, this has not hitherto been explored using Europium, even though Europium is popular fluorescent material. This may have been because conjugating Europium nanoparticles to antibody can functionally inactivate the antibody[37].

The currently optimized FICT can be easily exploited to apply Europium in RDTs for influenza virus and other diseases that require improved RDT sensitivity.

Virus infection could be diagnosed by immunofluorescence assay using fluorescent microscope. However, fluorescence microscopy requires the intensive high power light source including xenon, mercury or laser[38]. This light source limits the fluorescence microscopy to become a POCT.

Recently, modern smartphones are equipped with a lightweight, high-performance camera/imaging module, becoming the preferred tool for use in many POC applications[39, 40].

Therefore, the proposed fluorescent diagnostic system can contribute to the advance of the POCT diagnostic platform connected with modern smartphone-based diagnostic application.

BSA is a well-known blocker used to suppress non-specific reactions in an immunoassay[41]. pH can cause structural change of HA of influenza virus[42]. Therefore, we tested different pHs to find a more suitable condition of our FICT assay employing 6D7, which recognizes conformational structure of the HA1 epitope of H7 subtypes. H1N1 cross-reaction was suppressed by increasing pH, indicating that a non-physiologic pH could be efficient in discriminating HA subtypes. Antibody-antigen force is a weak interaction and the type of the weak
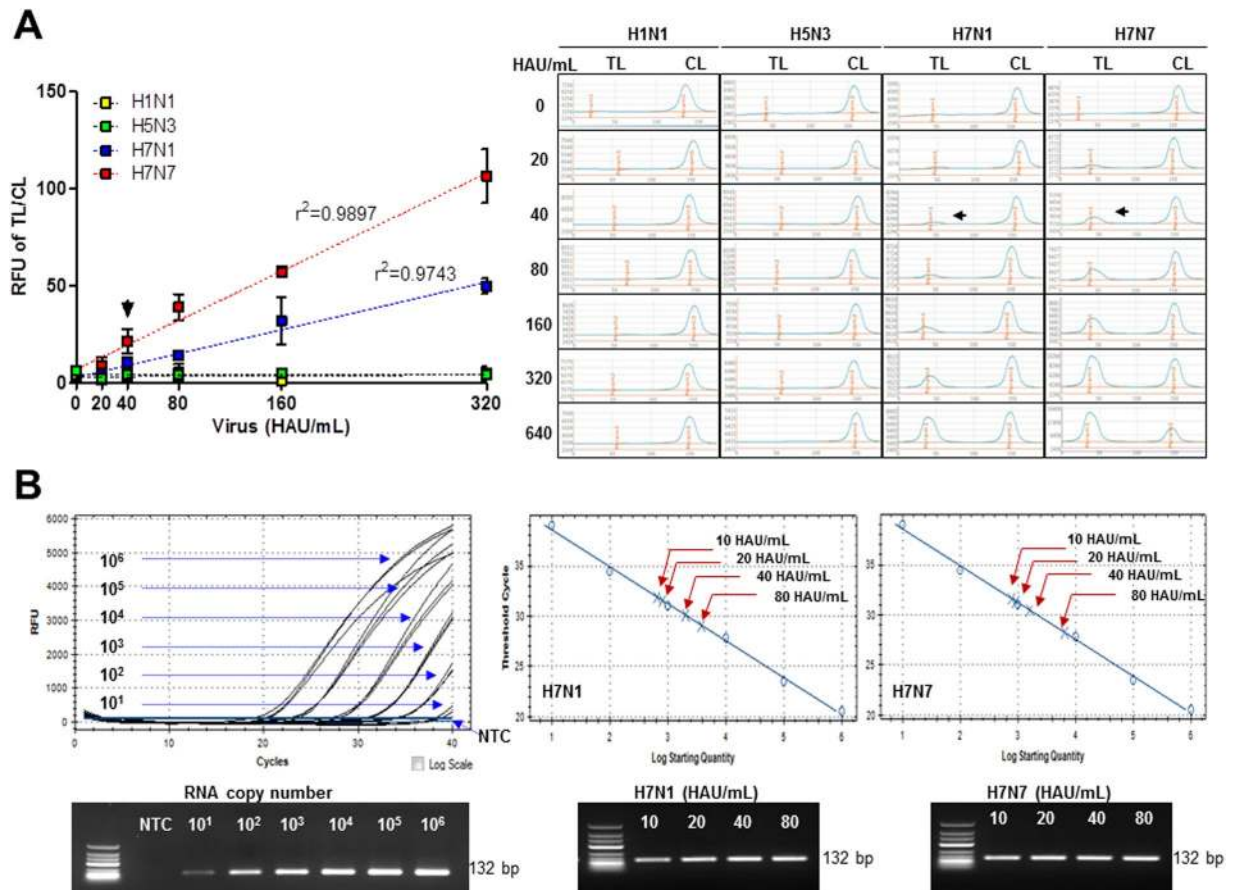
Figure 6. Assessment of FICT performance by rRT-PCR. Serially diluted virus (10–620 HAU/mL) was measured by FICT assay. The quantitative range of FICT assay was determined by linear regression using the GraphPad Prism 5.0 software, as shown by the dotted line (**A**). The black arrow indicates the virus titer of LOD of FICT assay. The data ($n = 3$) are shown as mean ± SD. Raw fluorescence peaks from the test line (TL) and control line (CL) in FICT are shown in right panel. FICT assay was compared with rRT-PCR (**B**). The linear relationship between the threshold cycle (Ct) and RNA copy number was shown. After preparing two-fold dilutions from of 10 HAU/mL to 80 PFU/mL of two H7 subtype viruses, sample was subjected to RNA extraction and used for rRT-PCR. Bottom panel shows the PCR product of different RNA for standard and each diluted virus from 10–80 HAU/mL. The red arrow indicates the point that corresponds to the RNA copy numbers and virus titer. NTC, no template control.

interaction is composed of Van der Waals force, hydrogen bond, hydrophobic interaction, and ion-dipole[43]. Weak interaction is involved in the epitope-paratope binding and a few amino acids is comprised in the specific binding[44]. Many factors influence antigen-antibody reaction and one of the factors affecting antigen-antibody reaction is pH[43]. Therefore, we consider that modification of pH may be a good way to fine-tune the conformational antigen-antibody reaction.

The Europium-based assay includes strip (cost: <$2 USD/test strip) and LED device (Medisensor Inc., Daegu, South Korea, cost: ~$20,000). As test kit is generally sold at a price of 20 USD/test kit[45], current Europium-based strip itself has a competition. Although the proposed assay requires an expensive reader, it still has advantage because device can be shared in one local area and reusable.

We tested the potential of performance in FICT with clinical samples by spiking virus and the proposed diagnostic method is considered to be useful as clinical application with human nasopharyngeal specimen (Figure S2). Our study is limited by the lack of data of human H7N9-infected patients, although a recombinant antigen of H7N9 HA1 could allow detection of H7N9 virus. The detection sensitivity and specificity of this assay needs to be evaluated when H7N9 patient samples are available.

In conclusion, novel H7 subtype-specific mAbs were developed and applied to a rapid fluorescent diagnostic system that incorporated Europium nanoparticles. The system displayed H7 subtype-specificity and enhanced H7 subtype virus detection sensitivity.

Methods

Reagents. Europium nanoparticles were purchased from Bangs Laboratories Inc. (Fishers, IN, USA). Aliphatic amine latex Beads (100 nm diameter) were purchased from Life Technology (Carlsbad, CA, USA). N-(3-Dimethylaminopropyl)-N′-ethylcarbodiimide hydrochloride (EDC) and N-hydroxysulfosuccinimide
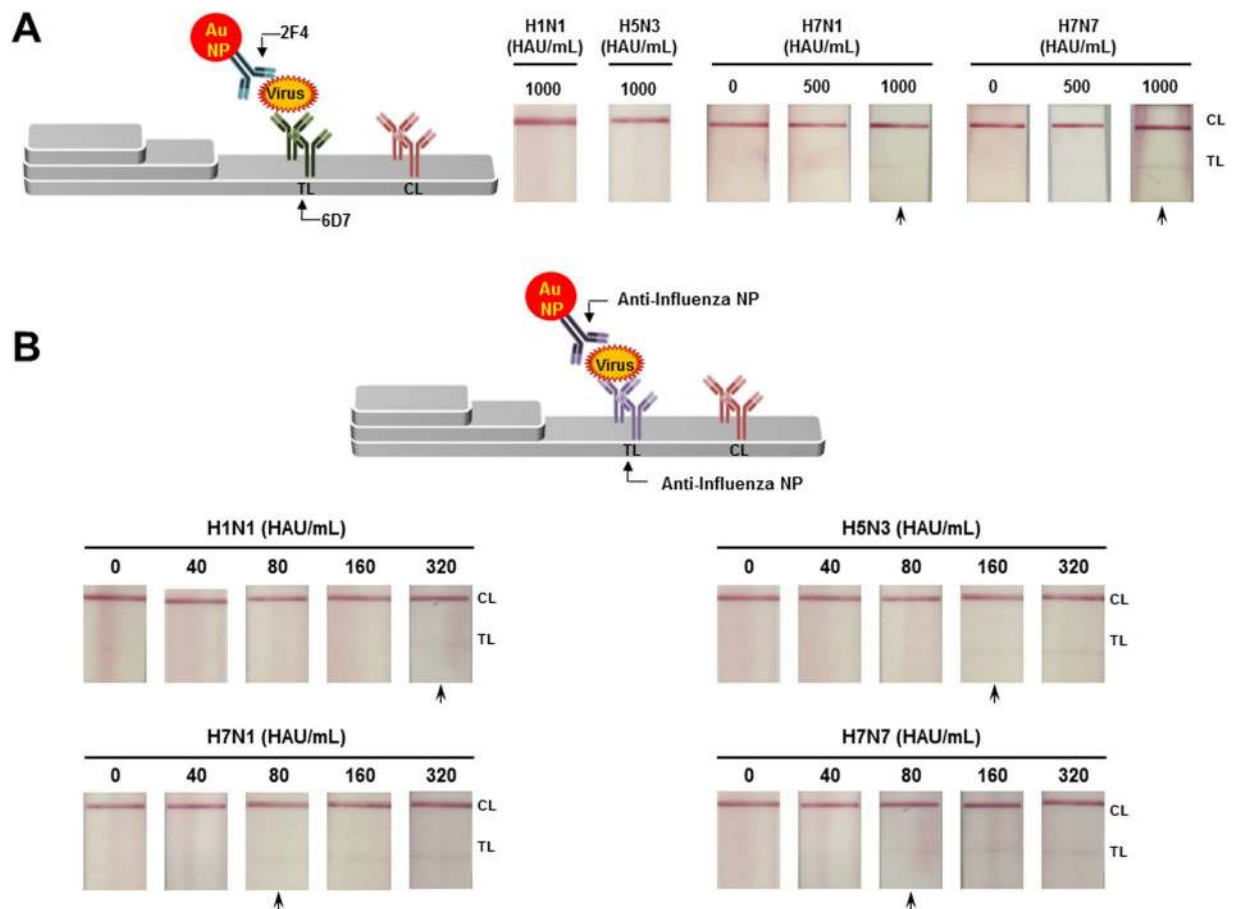
Figure 7. Limit of detection of conventional RDT. The 2F4 mAb conjugated with colloidal gold nanoparticle (Au NP) was captured on the TL (6D7mAb) if there was virus during lateral flow reaction. After 20 min, the strip was read with the naked eye for a binary decision. Two non-H7 subtype viruses (H1N1 and H5N3) were applied in high titer (1,000 HAU/mL) and for two H7 subtype virus (H7N1 and H7N7), 500 and 1,000 HAU/mL of each virus were applied to RDT (**A**). Conventional influenza A RDT targeting influenza A nucleoprotein (NP) was tested with the two-fold serially diluted four subtype virus from 40 to 80 HAU/mL (**B**). The arrow indicates the LOD.

sodium salt (Sulfo-NHS) were purchased from Thermo Scientific (Waltham, MA, USA). All other chemicals were purchased from Sigma-Aldrich (St. Louis, MO, USA) without further purification. Recombinant hemagglutinin 1 (rHA1) of H7N9 (A/Anhui/1/2013) and rHA1 of H5N1 (A/Vietnam/1/2003) were purchased from Sino Biological Inc. (Beijing, China). Anti-influenza A nucleoprotein (NP) (Clone 3G6) was provided by Professor Ho-Joon Shin, Ajou University, Suwon, Republic of Korea. Polyclonal goat anti-mouse IgG was purchased from Sigma-Aldrich.

Cell and virus.   Madin – Darby Canine Kidney (MDCK, NBL-2, ATCC® CCL-34™) cells was purchased from American Type Culture Collection (ATCC, Manassas, VA, USA). H1N1 was purchased from Korea Center for Disease Control and Prevention. AI virus (H5N3, H7N1, and H7N7) were kindly provided from Professor Haan Woo Sung, Kangwon National University, Chuncheon, Republic of Korea. The egg-cultured virus stock was titrated by HA assay and plaque assays were performed as previously described[22, 46].

Production and characterization of mAbs.   H7N9 (A/Anhui/1/2013) recombinant HA 1 (rHA1) (50 μg/100 μL) was mixed with an equal volume of Freund's complete adjuvant (Sigma-Aldrich) and injected intraperitoneally into a 6-week-old female BALYSIS BUFFER/c mice (Daehan Bio-Link, Eumseong, Korea). Boosts consisted of the H7N9 rHA1 protein (25 μg/100 μL) mixed with an equal volume of Freund's incomplete adjuvant biweekly. After the third boost, adjuvant-free H7N9 rHA1 (5 μg/100 μL) was injected intravenously. The cell fusion technique was previously described[47]. In brief, after confirmation of the Ab in mouse serum, splenocytes were extracted from a selected immune mouse and fused with myeloma cell (F/0 cell line) at a ratio of 1:5 to 1:1 in 50% polyethylene glycol and then seeded in each well of a 96-well culture plate. Hybridoma cells were selected by subculture in HAT (hypoxanthine, aminopterin, and thymidine) and HT (hypoxanthine and thymidine) media in a 5% CO_2 incubator at 37 °C for 2 weeks. After colonies appeared in each well, Ab titers were determined by an enzyme-linked immunosorbent assay (ELISA). Hybridoma cells producing mAb were selected by ELISA and cultured with a complete DMEM in a 24-well culture plate. For scaled-up mAb

production, mAb-producing cells were intraperitoneally injected into a 10-week-old female BALYSIS BUFFER/c mouse. Two weeks later, mouse ascites were collected and centrifuged at 5,000 × g for 15 min. The purified mAb from the ascites was obtained using a protein A agarose column (Amersham Biosciences, Uppsala, Sweden) and identified by Western blotting. For examination of the mAb isotypes, an Immunotype™ mouse monoclonal antibody isotyping kit (Sigma-Aldrich) was used.

Indirect ELISA assay.   Indirect ELISA was performed as describe previously[46]. Briefly, the purified antigen or virus were diluted in 50 mM bicarbonate/carbonate coating buffer (pH 9.6) and 75 μL of sample were prepared and used to coat wells of a 96-well microtitre plate were prepared and used to coat wells of a 96-well microtitre plate (Greiner, Germany) 37 °C for 2 h. The plate was washed with 200 μL of PBS, 0.1% Tween 20 (PBS-T, pH 7.4) and then blocked with 5% non-fat dry milk at 37 °C for 2 h. To react the antibody, in case of recombinant antigen-mediated ELISA, pre-immune sera derived from healthy mice (0.5 μL of sera/100 μL/well) and mAb (1 μg/100 μL/well) were added to each well, respectively. In case of virus detection, mAbs (2 μg/100 μL/well) were added to each well and positive control (anti-influenza A NP, 2 μg/100 μL/well) to convince the each subtype virus per well were added to each well and incubated at 37 °C to detect antigens. After 1 h, secondary Ab in the form of horseradish peroxidase (HRP)-conjugated rabbit anti-mouse IgG (Abcam, Cambridge, UK) was added to each well according to the manufacture's protocol. Stringent washing with PBS-T was performed five times to remove nonspecific biding and 100 μL of 3,3′,5,5′-tetra methyl benzidine (Sigma-Aldrich) substrate solution was added.

Western blot analysis.   The four subtype virus (H5N, H1N1, H7N1, and H7N7) were subjected to 12% SDS-PAGE and a running gel at 100 V for 2 h. The gel was soaked in transfer buffer, and the resolved proteins were transferred to a polyvinylidene difluoride membrane. The membrane was blocked with 5% non-fat milk for 2 h at 37 °C and each antibody diluted to a concentration of 10 μg/mL was added for 1 h. The HRP-conjugated antibody was used for detection according to the manufacturer's protocol. Anti-influenza NP (Clone 3G6) was used for loading control of each virus. Finally, Clarity Western ECL substrate (Bio-Rad, Hercules, CA, USA) was used to visualize the band using the ChemiDoc MP System (Bio-Rad).

IFA.   IFA was performed as described previously[48]. The first day, MDCK cells were coating on glass coverslips positioned in wells of a 6well plate and incubated at 37 °C overnight in an atmosphere of 5% CO_2. The next day, cells were infected at a multiplicity of infection of 0.5 in DMEM containing 1% antibiotic, 0.3% BSA and 1 μg/mL trypsin from bovine pancreas for 12 h, 37 °C, and 5% CO_2. Using fresh 4% paraformaldehyde in PBS (pH 6.9), cells were fixed for 15 min and after washing three times with 0.1% Tween 20 in PBS, a solution of 0.1% Triton X-100 was added to each well for permeabilization. Subsequently, cells were blocked with 5% BSA and 0.1% Tween 20 in PBS for 2 h at room temperature. To detect virus, mAbs (2F4 and 6D7) diluted 1:5000 in blocking buffer (0.5 μg/mL) were used. Subsequently, fluorescein isothiocyanate (FITC)-conjugated rabbit anti-mouse IgG secondary antibody was incubated for 1 h at room temperature. Finally, each coverslip was mounted on a slide including mounting medium and 4′,6-diamidino-2-phenylindole (DAPI; Vector Laboratories, Burlingame, CA, USA). Images of fluorescent cells were acquired with a fluorescence microscope (Olympus, Tokyo, Japan) using a 400× objective. Anti-influenza NP (3G6) was used as positive control antibody.

Conjugation of Europium nanoparticle.   Briefly, antibody was covalently conjugated to Europium by a well-established procedure from Bangs Laboratories. Briefly, 10 μL Europium (0.2 μm, 1% w/t) was added to 500 μL 0.1 M Tris-HCl (pH 7.0) and incubated for 1 h at 25 °C in the presence of 0.13 mM carbodiimide (EDC) and 10 mM Sulfo-N-hydroxysulfosuccinimide (Sulfo-NHS). EDC and Sulfo-NHS surplus was removed by centrifugation at 27,237 × g for 5 min. The activated Europium was mixed with 30 μL 10 μM Ab (2F4) in 500 μL 0.1 M sodium phosphate (pH 8.0) and allowed to react for 2 h at 30 °C. After centrifugation at 27,237 × g for 5 min, the Europium-conjugated antibody was collected, washed with 2 mM PBS (pH 8.0), resuspended in 100 μL storage buffer (1% BSA in PBS) and stored at 4 °C.

Lateral flow test strips for fluorescent immunochromatographic test (FICT).   The test strips used consisted of four components: sample application pad, conjugate pad, nitrocellulose (NC) membrane and absorbent pad. The test line (TL) of the strip was prepared by dispensing a desired volume of 2.5 mg/mL mouse monoclonal (anti-influenza H7 subtype-specific mAb; 6D7) and 0.5 mg/ml polyclonal goat anti-mouse IgG on the control line (CL). The diagnostic strip was tested after drying the membrane at 30 °C for 2 days. To select the pair antibody, a dot-FICT assay was used. Briefly, Ab (0.1 μg/μL) was dotted on a NC membrane lacking a TL and dried at 30 °C for 2 days. To perform the FICT assay, 2 μL of Europium-conjugated 2F4 Ab from a stock solution was dropped onto conjugate pad and a mixture of 75 μL of samples with 75 μL of lysis buffer (100 mM Tris-HCl, pH 9.0, 0.025 M EDTA, 0.5% sodium deoxycholate, and 1% Triton X- 100) were dropped onto sample pad for 15 minutes. The results of test strips were read with a portable fluorescent strip reader at excitation and emission wavelengths of at 355 nm and 612 nm, respectively (Medisensor, Daegu, South Korea)[49]. Both TL and CL signals were measured and the TL/CL ratio was calculated automatically.

Real-time RT-PCR (rRT-PCR).   rRT-PCR was performed using a Quantitect Probe RT-PCR Kit (QIAGEN, Hilden, Germany) to determine the cycle threshold (Ct) values using a CFX96 Real-Time PCR Detection System (Bio-Rad, Hercules, CA). The H7 primers, probes, and RT- PCR condition were described previously[34]. For standard of RNA copy number, the template was generated in plasmid pGEM-T Easy (Promega, Madison, WI, USA) including a 132 base pair (bp) HA1 insert. *In vitro* transcription of HA1 RNA used a RiboMax (Promega) kit to determine the RNA copy number for the limit of detection of FICT. The standard curve was calculated automatically by plotting the Ct values against each standard of known RNA copy number and by extrapolating the linear regression line of this curve. The PCR products were analyzed in agarose gels (2%).

Colloidal gold-based RDT assay.   To evaluate the performance of FICT assay, colloidal gold nanoparticles conjugated to Ab was prepared as previously described[50]. After 0.02% chloroauric acid (HAuCl4·4H$_2$O) (Sigma-Aldrich) was brought to a boil, 0.2% sodium citrate was added with constant stirring. After the mixture changed to a wine-reddish color, the solution was boiled for additional 5 min and then stirring for 10 min without boiling. Next, 1 mg of the mAb (2F4) was conjugated with the prepared colloidal gold particles (100 mL). The mAb-gold conjugate was precipitated by centrifugation (27,237 × g) and resuspended in PBS containing 0.1% of BSA to an optical density at 450 nm (OD$_{450}$) of 10. The TL of the strip was prepared by dispensing a desired volume of 2.5 mg/mL mouse mAb (6D7) and 0.5 mg/ml IgG mouse on the CL. Same lysis buffer was used for RDT. A commercial influenza virus A/B RDT (Standard Diagnostics, Yongin, South Korea) was used for comparison. Samples were applied following the manufacturer's instructions.

Ethical statement.   The study was approved by the Institutional Review Board of the Wonkwang University Hospital (Approval No. WKUH201607-HRBR-078) and all methods were carried out in accordance with relevant guidelines and regulations.

Statistics.   The mean ± standard deviation (SD) was calculated and all data were plotted using GraphPad Prism 5.0 (Graphpad, La Jolla, CA, USA).

References

1. CDC. Avian Influenza A (H7N9) Virus. https://www.cdc.gov/flu/avianflu/h7n9-virus.htm (2013).
2. Du Ry van Beest Holle, M., Meijer, A., Koopmans, M. & de Jager, C. M. Human-to-human transmission of avian influenza A/H7N7, The Netherlands, 2003. *Euro. Surveill.* **10**, 264–268 (2005).
3. Bos, M. E. *et al.* High probability of avian influenza virus (H7N7) transmission from poultry to humans active in disease control on infected farms. *J. Infect. Dis.* **201**, 1390–1396 (2010).
4. de Jong, M. C., Stegeman, A., van der Goot, J. & Koch, G. Intra- and interspecies transmission of H7N7 highly pathogenic avian influenza virus during the avian influenza epidemic in The Netherlands in 2003. *Rev. Sci. Tech.* **28**, 333–340 (2009).
5. Koopmans, M. *et al.* Transmission of H7N7 avian influenza A virus to human beings during a large outbreak in commercial poultry farms in the Netherlands. *Lancet.* **363**, 587–593 (2004).
6. Puzelli, S. *et al.* Human infection with highly pathogenic A(H7N7) avian influenza virus, Italy, 2013. *Emerg. Infect. Dis.* **20**, 1745–1749 (2014).
7. Bonfanti, L. *et al.* Highly pathogenic H7N7 avian influenza in Italy. *Vet. Rec.* **174**, 553–553 (2014).
8. Chen, E. *et al.* Human infection with avian influenza A(H7N9) virus re-emerges in China in winter 2013. *Euro. Surveill.* **18**, pii: 20616 (2013).
9. William, T. *et al.* Avian influenza (H7N9) virus infection in Chinese tourist in Malaysia, 2014. *Emerg. Infect. Dis.* **21**, 142–145 (2015).
10. Yu, H. *et al.* Human infection with avian influenza A H7N9 virus: an assessment of clinical severity. *Lancet.* **382**, 138–145 (2013).
11. Sutton, T. C. *et al.* Airborne transmission of highly pathogenic H7N1 influenza virus in ferrets. *J. Virol.* **88**, 6623–6635 (2014).
12. Fouchier, R. A. *et al.* Avian influenza A virus (H7N7) associated with human conjunctivitis and a fatal case of acute respiratory distress syndrome. *Proc. Natl. Acad. Sci. USA* **101**, 1356–1361 (2004).
13. Richard, M. *et al.* Limited airborne transmission of H7N9 influenza A virus between ferrets. *Nature.* **501**, 560–563 (2013).
14. Xiang, N. *et al.* Comparison of the first three waves of avian influenza A(H7N9) virus circulation in the mainland of the People's Republic of China. *BMC Infect. Dis.* **16**, 734–734 (2016).
15. CDC. Diagnostics for Detecting H7N9 Using rRT-PCR. https://www.cdc.gov/flu/avianflu/h7n9/detecting-diagnostics.htm (2013).
16. Chen, Y. *et al.* Rapid diagnostic tests for identifying avian influenza A(H7N9) virus in clinical samples. *Emerg. Infect. Dis.* **21**, 87–90 (2015).
17. Kang, K. *et al.* Development of rapid immunochromatographic test for hemagglutinin antigen of H7 subtype in patients infected with novel avian influenza A (H7N9) virus. *PLoS One.* **9**, e92306, doi:10.1371/journal.pone.0092306 (2014).
18. Luan, J. *et al.* PEGylated artificial antibodies: plasmonic biosensors with improved selectivity. *ACS Appl. Mater. Interfaces.* **8**, 23509–23516 (2016).
19. Nutter, S. *et al.* Evaluation of indirect fluorescent antibody assays compared to rapid influenza diagnostic tests for the detection of pandemic influenza A (H1N1) pdm09. *PLoS One.* **7**, e33097, doi:10.1371/journal.pone.0033097 (2012).
20. Okubo, S., Cheung, M. & Adler-Shohet, F. C. Comparing indirect fluorescent antibody assays to rapid diagnostic tests for the detection of influenza A(H1N1)pdm09. *MLO Med. Lab. Obs.* **44**, 8–12 (2012).
21. Sakurai, A. *et al.* Fluorescent immunochromatography for rapid and sensitive typing of seasonal influenza viruses. *PLoS One.* **10**, e0116715, doi:10.1371/journal.pone.0116715 (2015).
22. Yeo, S. J. *et al.* Rapid and quantitative detection of zoonotic influenza A virus infection utilizing coumarin-derived dendrimer-based fluorescent immunochromatographic strip test (FICT). *Theranostics.* **4**, 1239–1249 (2014).
23. Zhang, P. *et al.* A highly sensitive europium nanoparticle-based immunoassay for detection of influenza A/B virus antigen in clinical specimens. *J. Clin. Microbiol.* **52**, 4385–4387 (2014).
24. Liu, J., Zhao, J., Petrochenko, P., Zheng, J. & Hewlett, I. Sensitive detection of influenza viruses with Europium nanoparticles on an epoxy silica sol-gel functionalized polycarbonate-polydimethylsiloxane hybrid microchip. *Biosens. Bioelectron.* **86**, 150–155 (2016).
25. Armbruster, D. A. & Pry, T. Limit of blank, limit of detection and limit of quantitation. *Clin. Biochem. Rev.* **29**, S49–52 (2008).
26. Zhong, C. *et al.* Determination of plasmid copy number reveals the total plasmid DNA amount is greater than the chromosomal DNA amount in Bacillus thuringiensis YBT-1520. *PLoS One.* **6**, e16025, doi:10.1371/journal.pone.0016025 (2011).
27. Velumani, S. *et al.* Development of an antigen-capture ELISA for detection of H7 subtype avian influenza from experimentally infected chickens. *J. Virol. Methods.* **147**, 219–225 (2008).
28. Shien, J. H. *et al.* Development of blocking ELISA for detection of antibodies against avian influenza virus of the H7 subtype. *J. Microbiol. Immunol. Infect.* **41**, 369–376 (2008).
29. Yang, M. *et al.* Evaluation of diagnostic applications of monoclonal antibodies against avian influenza H7 viruses. *Clin. Vaccine Immunol.* **17**, 1398–1406 (2010).
30. Mahmoudian, J. *et al.* Comparison of the photobleaching and photostability traits of Alexa Fluor 568- and fluorescein isothiocyanate-conjugated antibody. *Cell J.* **13**, 169–172 (2011).
31. Gravel, C. *et al.* Development and applications of universal H7 subtype-specific antibodies for the analysis of influenza H7N9 vaccines. *Vaccine.* **33**, 1129–1134 (2015).
32. Pedersen, J. *et al.* Validation of a real-time reverse transcriptase-PCR assay for the detection of H7 avian influenza virus. *Avian Dis.* **54**, 639–643 (2010).
33. Spackman, E. *et al.* Development of a real-time reverse transcriptase PCR assay for type A influenza virus and the avian H5 and H7 hemagglutinin subtypes. *J. Clin. Microbiol.* **40**, 3256–3260 (2002).

34. Slomka, M. J. *et al.* Validated real-time reverse transcriptase PCR methods for the diagnosis and pathotyping of Eurasian H7 avian influenza viruses. *Influenza Other Respir. Viruses.* **3**, 151–164 (2009).
35. He, F. *et al.* Development of dual-function ELISA for effective antigen and antibody detection against H7 avian influenza virus. *BMC Microbiol.* **13**, 219 (2013).
36. Moreira, E. A. *et al.* A conserved influenza A virus nucleoprotein code controls specific viral genome packaging. *Nat. Commun.* **7**, 12861, doi:10.1038/ncomms12861 (2016).
37. Werthen, M. & Nygren, H. Effect of antibody affinity on the isotherm of antibody binding to surface-immobilized antigen. *J. Immunol. Methods.* **115**, 71–78 (1988).
38. Sanderson, M. J., Smith, I., Parker, I. & Bootman, M.D. Fluorescence microscopy. Cold Spring Harb Protoc. pdb.top071795, doi:10.1101/pdb.top071795 (2014).
39. Liu, X., Lin, T. Y. & Lillehoj, P. B. Smartphones for cell and biomolecular detection. *Ann. Biomed. Eng.* **42**, 2205–2217 (2014).
40. Yeo, S. J., Cuc, B. T., Sung, H. W. & Park, H. Evaluation of a smartphone-based rapid fluorescent diagnostic system for H9N2 virus in specific-pathogen-free chickens. *Arch. Virol.* **161**, 2249–56 (2016).
41. Xiao, Y. & Isaacs, S. N. Enzyme-linked immunosorbent assay (ELISA) and blocking with bovine serum albumin (BSA)–not all BSAs are alike. *J. Immunol. Methods.* **384**, 148–151 (2012).
42. Fontana, J., Cardone, G., Heymann, J. B., Winkler, D. C. & Steven, A. C. Structural changes in Influenza virus at low pH characterized by cryo-electron tomography. *J. Virol.* **86**, 2919–2929 (2012).
43. Reverberi, R. & Reverberi, L. Factors affecting the antigen-antibody reaction. *Blood Transfus.* **5**, 227–40 (2007).
44. Van Oss, C. J. Hydrophobic, hydrophilic and other interactions in epitope-paratope binding. *Mol. Immunol.* **32**, 199–211 (1995).
45. Ley, B. *et al.* Evaluation of a rapid dipstick (Crystal VC) for the diagnosis of cholera in Zanzibar and a comparison with previous studies. *PLoS One.* **7**, e36930, doi:10.1371/journal.pone.0036930 (2012).
46. Yeo, S. J. *et al.* Smartphone-based fluorescent diagnostic system for highly pathogenic H5N1 viruses. *Theranostics.* **6**, 231–242 (2016).
47. Kim, J. H. *et al.* Production of monoclonal antibodies for Plasmodium vivax lactate dehydrogenase and patient sera screening using sandwich ELISA. *Parasitol. Res.* **111**, 1645–1650 (2012).
48. Yeo, S. J. *et al.* Potential Interaction of *Plasmodium falciparum* Hsp60 and Calpain. *Korean J. Parasitol.* **53**, 665–673 (2105).
49. Ham, J. Y. *et al.* Highly sensitive and novel point-of-care system, aQcare Chlamydia TRF kit for detecting Chlamydia trachomatis by using europium (Eu) (III) chelated nanoparticles. *Ann. Lab. Med.* **35**, 50–56 (2015).
50. Liu, X. *et al.* Colloidal gold nanoparticle probe-based immunochromatographic assay for the rapid detection of chromium ions in water and serum samples. *Anal. Chim. Acta.* **745**, 99–105 (2012).

Acknowledgements

Author Contributions

S.J. and D.T.B. developed dot-FICT and performed FICT assay to find the suitable pair of mAbs under the guidance of H.P. G.E. and H.J. Sohn developed mAbs under H.J. Shin. B.T., N.T.V., T.T., and N.T.P. performed FICT immunoassay for optimization. S.J. and D.T.H. conducted rRT-PCR and analyzed data. C.K. developed the Au-NP-based R.D.T. with novel mAbs. S.J., H.J. Shin, and H.P. wrote the paper with inputs from all other authors.

Additional Information

Supplementary information accompanies this paper at doi:10.1038/s41598-017-08328-9

Competing Interests: The authors declare that they have no competing interests.

Publisher's note: Springer Nature remains neutral with regard to jurisdictional claims in published maps and institutional affiliations.